

DFT Investigation of Structural, Electronic, and Catalytic Properties of Diiron Complexes Related to the $[2\text{Fe}]_{\text{H}}$ Subcluster of Fe-Only Hydrogenases

Maurizio Bruschi,[†] Piercarlo Fantucci,[‡] and Luca De Gioia^{*‡}

Department of Environmental Sciences and Department of Biotechnology and Biosciences,
University of Milan-Bicocca, Piazza della Scienza 2, I-20156 Milan, Italy

Received July 20, 2001

Hydrogenases catalyze the reversible oxidation of dihydrogen to protons and electrons. The structures of two Fe-only hydrogenases have been recently reported [Peters, J. W.; Lanzilotta, W. N.; Lemon, B. J.; Seefeldt, L. C. *Science* **1998**, *282*, 1853–1858. Nicolet, Y.; Piras, C.; Legrand, P.; Hatchikian, E. C.; Fontecilla-Camps, J. C. *Structure* **1999**, *7*, 13–23], showing that the likely site of dihydrogen activation is the so-called $[2\text{Fe}]_{\text{H}}$ cluster, where each Fe ion is coordinated by CO and CN^- ligands and the two metals are bridged by a chelating $\text{S}-\text{X}_3-\text{S}$ ligand. Moreover, the presence of a water molecule coordinated to the distal Fe2 center suggested that the Fe2 atom could be a suitable site for binding and activation of H_2 . In this contribution, we report a density functional theory investigation of the structural and electronic properties of complexes derived from the $[(\text{CO})(\text{CH}_3\text{S})(\text{CN})\text{Fe}(\text{II})(\mu\text{-PDT})\text{Fe}(\text{II})(\text{CO})_2(\text{CN})]^{-1}$ species, which is related to the $[2\text{Fe}]_{\text{H}}$ cluster observed in Fe-only hydrogenases. Our results show that the structure of the $[2\text{Fe}]_{\text{H}}$ cluster observed in the enzyme does not correspond to a stable form of the isolated cluster, in the absence of the protein. As a consequence, the reactivity of $[(\text{CO})(\text{CH}_3\text{S})(\text{CN})\text{Fe}(\text{II})(\mu\text{-PDT})\text{Fe}(\text{II})(\text{CO})_2(\text{CN})]^{-1}$ derivatives in solution may be expected to be quite different from that of the active site of Fe-only hydrogenases. In fact, the most favorable path for H_2 activation involves the two metal atoms and one of the bridging S atoms and is associated with a very low activation energy ($5.3 \text{ kcal mol}^{-1}$). The relevance of these observations for the catalytic properties of Fe-only hydrogenases is discussed in light of available experimental and theoretical data.

Introduction

Hydrogenases are enzymes that catalyze the reversible oxidation of dihydrogen to protons and electrons.¹ The structure of two Fe-only hydrogenases has been recently reported: the monomeric, cytoplasmic hydrogenase (CpI) from the anaerobic microorganism *Clostridium pasteurianum*² and the dimeric, periplasmic hydrogenase (DdH) from the sulfate-reducing microorganism *Desulfovibrio desulfuricans*.³ The two enzymes are highly related, and the domains associated with the active sites are structurally very similar.⁴

Of particular interest are the structural features of the active site (the so-called H cluster), which is formed by a regular $[4\text{Fe}-4\text{S}]_{\text{H}}$ cluster that is presumably involved in electron transfer and bridged by a cysteine residue to the $[2\text{Fe}]_{\text{H}}$ subcluster. This subcluster is the likely site of dihydrogen activation. The two iron atoms of $[2\text{Fe}]_{\text{H}}$ are coordinated by CO and CN^- ligands and bridged by a chelating $\text{S}-\text{X}_3-\text{S}$ ligand, where X_3 is composed of covalently linked light atoms. The $\text{S}-\text{X}_3-\text{S}$ ligand could be 1,3-propanedithiol (PDT),³ but other combinations of C, N, or O atoms would be consistent with crystallographic data. Moreover, the particular coordination environment of distal Fe2, with a coordination position vacant in DdH and occupied by a water molecule in CpI, is considered a suitable binding site for H_2 (see Figure 1a).

* Corresponding author. E-mail: luca.degioia@unimib.it. Fax: +39 02 64483478.

[†] Department of Environmental Sciences.

[‡] Department of Biotechnology and Biosciences.

(1) Albracht, S. P. J. *Biochim. Biophys. Acta* **1994**, *90*, 167–204. Adams, M. W. W. *Biochim. Biophys. Acta* **1990**, *1020*, 115–145.

(2) Peters, J. W.; Lanzilotta, W. N.; Lemon, B. J.; Seefeldt, L. C. *Science* **1998**, *282*, 1853–1858.

(3) Nicolet, Y.; Piras, C.; Legrand, P.; Hatchikian, E. C.; Fontecilla-Camps, J. C. *Structure* **1999**, *7*, 13–23.

(4) Peters, J. W. *Curr. Opin. Struct. Biol.* **1999**, *9*, 670–676. Nicolet, Y.; Lemon, B. J.; Fontecilla-Camps, J. C.; Peters, J. W. *Trends Biochem. Sci.* **2000**, *25*, 138–143.

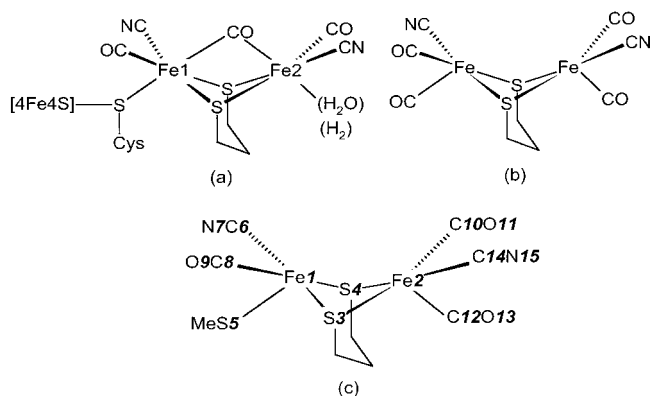


Figure 1. (a) Schematic structure of the $[2\text{Fe}]_{\text{H}}$ cluster, as deduced by X-ray diffraction.^{2,3} The weakly bound H_2O molecule, which is coordinated to the putative site of H_2 binding, is shown in brackets. (b) Schematic structure of the synthetic complex $[(\mu\text{-SCH}_2\text{CH}_2\text{CH}_2\text{S})\text{Fe}_2(\text{CO})_4(\text{CN})_2]^{-2}$ (**1**).⁷ (c) Schematic structure of the $[(\text{CO})(\text{CH}_3\text{S})(\text{CN})\text{Fe}(\mu\text{-PDT})\text{Fe}(\text{CO})_2(\text{CN})]^{-1}$ complex investigated in the present work. Atoms are numbered in agreement with Tables 3, 4, and 5.

The fully oxidized and reduced forms of the enzyme are EPR silent, while the partially oxidized form is paramagnetic.⁵ However, the oxidation state of the $[2\text{Fe}]_{\text{H}}$ cluster in various redox states is still controversial. For instance, Popescu and Munck⁶ suggest that the fully reduced state of the enzyme is a low-spin $\text{Fe}(\text{II})\text{Fe}(\text{II})$ species, while the partially oxidized form could be of a mixed-valence $\text{Fe}(\text{III})\text{-Fe}(\text{II})$ type. However, the Mossbauer data are also compatible with an $\text{Fe}(\text{I})\text{Fe}(\text{I})/\text{Fe}(\text{I})\text{Fe}(\text{II})$ redox couple. Recently, three research groups⁷ have independently reported the synthesis and characterization of the $\text{Fe}(\text{I})\text{Fe}(\text{I})$ complex $[(\mu\text{-PDT})\text{Fe}_2(\text{CO})_4(\text{CN})_2]^{-2}$ (**1**) (see Figure 1b). The similarity between **1** and the active site of Fe-only hydrogenases suggests that the reduced form of the enzyme is compatible with an $\text{Fe}(\text{I})\text{Fe}(\text{I})$ redox state. However, complex **1** does not exhibit catalytic properties toward H_2 . Kubas and co-workers⁸ reported H_2 activation on highly electrophilic organometallic complexes containing CO ligands, suggesting that the heterolytic cleavage of H_2 in Fe-only hydrogenases takes place on a low-spin $\text{Fe}(\text{II})$ center. Theoretical calculations, carried out on models based on the X-ray structure of the $[2\text{Fe}]_{\text{H}}$ subcluster, led to the conclusion that only an $\text{Fe}(\text{II})\text{-Fe}(\text{II})$ species can promote H_2 dissociation.⁹ However, these calculations showed also that when H_2 binds to the Fe2 center and replaces the H_2O molecule (see Figure 1a) and the $\text{S-X}_3\text{-S}$ ligand is a PDT moiety the reaction is kinetically or thermodynamically hindered. Interestingly, a recent reinvestigation of the X-ray structure of the Fe-only hydrogenase from *D. desulfuricans*¹⁰ has led to the proposal (not

yet verified experimentally) that the ligand bridging the two Fe atoms is a di(thiomethyl)amine molecule (DTMA). In this context, Hall and co-workers¹¹ have recently shown, using density functional theory (DFT) calculations, that the central N atom of DTMA may act as a base in H_2 activation, resulting in a slightly endothermic reaction ($2.6 \text{ kcal mol}^{-1}$) associated with a low activation barrier ($6.5 \text{ kcal mol}^{-1}$).

It is worth noting that these theoretical results are all based on the structure of the $[2\text{Fe}]_{\text{H}}$ subcluster, as observed by X-ray diffraction of the whole enzyme, and consequently start from the assumption that the terminal Fe2 site is the only coordination site suitable to bind H_2 . However, the situation can be different when considering isolated coordination compounds analogous to the $[2\text{Fe}]_{\text{H}}$ subcluster (see Figure 1). Besides, the experimental and theoretical investigations of organometallic complexes as biomimetic models of the Fe-only hydrogenase active site are useful for defining the steric and electronic factors of the isolated metallic cofactor and could help in designing new catalysts. All these considerations prompted us to carry out a DFT investigation of the structure and electronic properties of derivatives of the $\text{Fe}(\text{II})\text{Fe}(\text{II})$ organometallic complex $[(\text{CO})(\text{CH}_3\text{S})(\text{CN})\text{Fe}(\mu\text{-PDT})\text{Fe}(\text{CO})_2(\text{CN})]^{-1}$, which is related to the active site of Fe-only hydrogenases. Our aim was to investigate plausible reaction paths in H_2 activation. Computational results are compared with available theoretical and experimental data obtained from model complexes and from the native enzyme.

Methods

DFT calculations were carried out using the hybrid B3LYP exchange–correlation functional¹² and the effective atomic core potential derived by Hay and Wadt¹³ for iron and sulfur atoms. The adopted basis set is of the augmented double- ζ type: one set of f polarization functions and one set of d functions was added to Fe and S atoms, respectively.¹⁴ All other atoms were described by the double- ζ basis set at the all-electron level.¹⁵ For the reactive hydrogens, the double- ζ basis set was augmented by a set of standard p functions.

Stationary points on the energy hypersurface have been located by means of energy-gradient techniques. In particular, transition-state (TS) structures have been optimized using the synchronous transit quasi-Newton method,¹⁶ as implemented in the Gaussian 98 set of programs.¹⁷ A full vibrational analysis has been performed to further characterize each stationary point.

The optimized structures of the complexes reported in the present study correspond to diamagnetic low-spin states; high-spin states

- (5) Pierik, A. J.; Hagen, W. R.; Redeker, J. S.; Wolbert, R. B. G.; Boersma, M.; Verhagen, M. F. J. M.; Grande, H. J.; Veeger, C.; Mutsaers, P. H.; Sand, R. H.; Dunham, W. R. *Eur. J. Biochem.* **1992**, *209*, 63–71.
- (6) Popescu, C. V.; Munck, E. *J. Am. Chem. Soc.* **1999**, *121*, 7877–7884.
- (7) (a) Lyon, E. J.; Georgakaki, I. P.; Reibenspies, J. H.; Darensbourg, M. Y. *Angew. Chem., Int. Ed.* **1999**, *38*, 3178–3180. (b) Schmidt, M.; Contakes, S. M.; Rauchfuss, T. B. *J. Am. Chem. Soc.* **1999**, *121*, 9736–9737. (c) Le Cloiret, A.; Best, S. P.; Borg, S.; Davies, S. C.; Evans, D. J.; Hughes, D. L.; Pickett, C. J. *Chem. Commun.* **1999**, *22*, 2285–2286.
- (8) Huhmann-Vincent, J.; Scott, B. L.; Kubas, G. J. *Inorg. Chim. Acta* **1999**, *294*, 240–247.
- (9) Cao, Z.; Hall, M. B. *J. Am. Chem. Soc.* **2001**, *123*, 3734–3742.

- (10) Nicolet, Y.; de Lacey, A. L.; Vernède, X.; Fernandez, V. M.; Hatchikian, E. C.; Fontecilla-Camps, J. C. *J. Am. Chem. Soc.* **2001**, *123*, 1596–1601.
- (11) Fan, H.-J.; Hall, M. B. *J. Am. Chem. Soc.* **2001**, *123*, 3828–3829.
- (12) Becke, A. D. *Phys. Rev. A: At., Mol., Opt. Phys.* **1988**, *38*, 3098–3104. Becke, A. D. *J. Chem. Phys.* **1992**, *96*, 2155–2160. Becke, A. D. *J. Chem. Phys.* **1993**, *98*, 5648–5652. Stevens, P. J.; Devlin, F. J.; Chabrowski, C. F.; Frisch, M. J. *J. Phys. Chem.* **1994**, *98*, 11623–11627.
- (13) Hay, P. J.; Wadt, W. R. *J. Chem. Phys.* **1985**, *82*, 299–306.
- (14) Rassolov, V.; Pople, J. A.; Ratner, M.; Windus, T. L. *J. Chem. Phys.* **1998**, *109*, 1223.
- (15) Dunning, H., Jr.; Hay, P. J. In *Methods of Electronic Structure Theory*; Schaefer, H. F., III, Ed.; Plenum Publishing: New York, 1977; Vol. 3.
- (16) Peng, C.; Schlegel, H. B. *Isr. J. Chem.* **1994**, *33*, 449–458.

Table 1. Experimentally Observed and Computed Structural Parameters for the Complex $[(\mu\text{-SCH}_2\text{CH}_2\text{CH}_2\text{S})\text{Fe}_2(\text{CO})_4(\text{CN})_2]^{-2}$

	X-ray data ^a	present work ^b	Hall et al. ^c
Fe—CO _{eq}	1.741	1.761	1.753
Fe—CO _{ax}	1.769	1.741	1.745
Fe—CN	1.929	1.931	1.927
Fe—S	2.266–2.269	2.324–2.345	2.334
Fe—Fe	2.517	2.555	2.544
CO—Fe—CO	98.8	103.65	
CO _{eq} —Fe—CN	90.1	89.00	
CO _{ax} —Fe—CN	98.3	93.41	
Fe—S—Fe	67.25	66.20	
S—Fe—S	85.74	86.14	

^a X-ray diffraction data of reference 7b. ^b DFT B3LYP calculations. ^c DFT B3LYP calculations from reference 9.

for the isomers of the parent compound $[(\text{CO})(\text{CH}_3\text{S})(\text{CN})(\text{H}_2\text{O})\text{Fe}(\mu\text{-PDT})\text{Fe}(\text{CO})_2(\text{CN})]^{-1}$ are higher in energy, as expected, considering the characteristics of the ligands forming the coordination environment of the metal atoms.

Results and Discussion

To check the reliability of the adopted computational scheme, we carried out geometry optimization of the Fe(I)-Fe(I) complex $[(\mu\text{-PDT})\text{Fe}_2(\text{CO})_4(\text{CN})_2]^{-2}$, hereafter referred as **1** (see Figure 1b), for which the experimental structure is known.⁷ The comparison between X-ray-derived and DFT-computed bond distances and valence angles for **1**, reported in Table 1, is satisfactory. The disagreement for bond distances is, in general, about 0.03 Å and for valence angles, about 5°. The computed bond distance with the largest deviation with respect to the experiment is for the Fe—S bond, which is consistently overestimated by our DFT treatment by about 0.07 Å. Such an error is present also in the DFT results of Hall et al.^{9,11} despite the larger basis set they adopted and is probably to be ascribed to limitations of the B3LYP exchange–correlation functional. Thus, the computed Fe—S distances are expected to be overestimated in all the complexes discussed in this contribution. However, this overestimation is not a serious drawback because it cannot substantially affect the general reliability of our computational scheme, in particular when it is applied to a systematic study of homologous complexes.

$[(\text{CO})(\text{CH}_3\text{S})(\text{CN})(\text{H}_2\text{O})\text{Fe}(\text{II})(\mu\text{-PDT})\text{Fe}(\text{II})(\text{CO})_2(\text{CN})]^{-1}$. X-ray diffraction experiments on the oxidized form of the enzyme² showed that an oxygen atom from a hydroxo group or a water molecule is coordinated to the Fe2 center of the $[\text{2Fe}]_{\text{H}}$ subcluster. Besides, water is considered to be a typical coordinating solvent, and the investigation of its interactions with the bimetallic cluster is relevant to under-

stand its chemical properties in solution. The Fe(II)Fe(II) complex $[(\text{CO})(\text{CH}_3\text{S})(\text{CN})(\text{H}_2\text{O})\text{Fe}(\mu\text{-PDT})\text{Fe}(\text{CO})_2(\text{CN})]^{-1}$ is expected to be a suitable model of the isolated hydrated $[\text{2Fe}]_{\text{H}}$ cluster (see Figure 1a), and to investigate its structural properties, we have carried out geometry optimizations that led to the identification of three isomers (referred as **2**, **3**, and **4**; see Figure 2). The net atomic charges for the three isomers, computed according to the natural atomic orbital (NAO) analysis,¹⁸ are collected in Table 2. It is noteworthy that in all isomers both metal atoms are characterized by partial charge values that are very close to zero, indicating the highly covalent nature of the metallic cluster. In complex **2**, the water molecule is coordinated to Fe1 and is trans to a CO ligand, the CH₃S group is trans to a bridging sulfur ligand, and the semibridged CO is close to Fe1 and interacts very weakly with Fe2 (Fe2—CO = 2.592 Å). In **3**, the water molecule is coordinated to Fe2 and is trans to a CO ligand that bridges the two metal centers asymmetrically, the CH₃S group is also trans to the bridging CO group, and the two iron atoms are both hexacoordinated. (Note, however, that the distance between Fe2 and the bridging CO is as long as 2.232 Å.) Interestingly, **3**, which is structurally related to the $[\text{2Fe}]_{\text{H}}$ subcluster observed in X-ray diffraction experiments on the oxidized form of Fe-only hydrogenases,² is 15.2 kcal mol⁻¹ less stable than **2**. In **4**, the water molecule is bridged between the two iron centers and is trans to the CH₃S ligand and the metal atoms are both hexacoordinated. This isomer is almost 10 kcal mol⁻¹ more stable than **3**. The difference in stability among the three isomers can be qualitatively explained by considering the electronic properties of the Fe—CO bonds. It is well-known¹⁹ that in metal–carbonyl complexes the metal–CO bonds are destabilized when CO is trans to π -acid groups. In fact, in **2**, two CO groups are trans to a sulfur atom (a weak π -acid group) and a water molecule (a strong σ -donating group), respectively, whereas the coordination position that is trans to the axial CO coordinated to Fe2 is vacant (see Figure 2). In **4**, the three CO groups are in trans to two S atoms and one water molecule, respectively. In the less stable **3**, the three CO groups are trans to S atoms, which lower the stability of the isomer because of their nonnegligible π acidity. Therefore, in light of X-ray data^{2,3} and present results and by assuming that the oxidized form of the enzyme corresponds to an Fe(II)Fe(II) redox state, the protein environment could destabilize **2** and **4** or make them kinetically inaccessible so that only **3** is observed in the enzyme. Actually, **2** does not fit inside the enzyme pocket, as deduced by a superposition experiment in which the CH₃S— group of **2** is forced to match the corresponding group of cysteine 382 in the enzyme (numbering of *D. desulfuricans* Fe hydrogenase; data not shown). As a result, the possible destabilization of **2** within the protein environment is not surprising, considering the steric properties of the active site. On the contrary, the steric and electronic factors responsible for the destabilization (or

(17) Frisch, M. J.; Trucks, G. W.; Schlegel, H. B.; Scuseria, G. E.; Robb, M. A.; Cheeseman, J. R.; Zakrzewski, V. G.; Montgomery, J. A., Jr.; Stratmann, R. E.; Burant, J. C.; Dapprich, S.; Millam, J. M.; Daniels, A. D.; Kudin, K. N.; Strain, M. C.; Farkas, O.; Tomasi, J.; Barone, V.; Cossi, M.; Cammi, R.; Mennucci, B.; Pomelli, C.; Adamo, C.; Clifford, S.; Ochterski, J.; Petersson, G. A.; Ayala, P. Y.; Cui, Q.; Morokuma, K.; Malick, D. K.; Rabuck, A. D.; Raghavachari, K.; Foresman, J. B.; Cioslowski, J.; Ortiz, J. V.; Stefanov, B. B.; Liu, G.; Liashenko, A.; Piskorz, P.; Komaromi, I.; Gomperts, R.; Martin, R. L.; Fox, D. J.; Keith, T.; Al-Laham, M. A.; Peng, C. Y.; Nanayakkara, A.; Gonzalez, C.; Challacombe, M.; Gill, P. M. W.; Johnson, B. G.; Chen, W.; Wong, M. W.; Andres, J. L.; Head-Gordon, M.; Replogle, E. S.; Pople, J. A. *Gaussian 98*; Gaussian, Inc.: Pittsburgh, PA, 1998.

(18) Reed, A. E.; Weinstock, R. B.; Weinhold, F. *J. Chem. Phys.* **1985**, *83*, 735.

(19) Cotton, F. A.; Wilkinson, G. *Advanced Inorganic Chemistry*, 5th ed.; Wiley & Sons: New York, 1988.

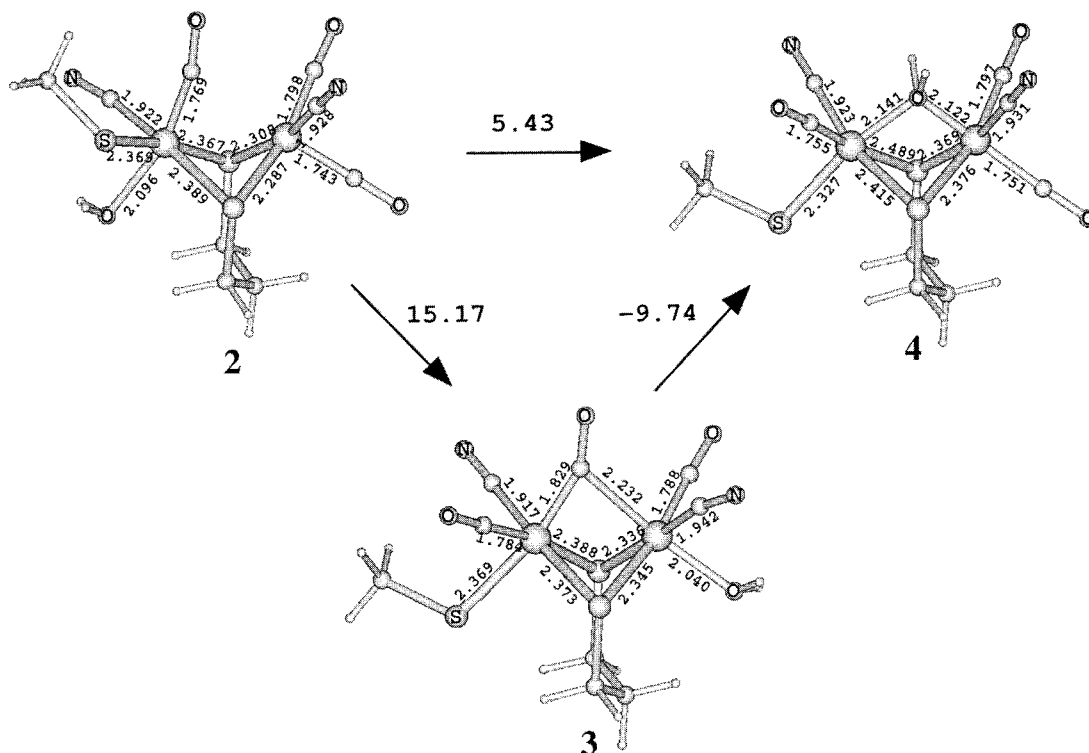


Figure 2. Optimized structures and relative energies of **2**, **3**, and **4**. Relevant bond distances are shown. Fe–Fe distances for **2**, **3**, and **4** are 2.653, 3.025, and 2.573 Å, respectively.

Table 2. Natural Atomic Charges of $[(\text{CO})(\text{CH}_3\text{S})(\text{CN})(\text{H}_2\text{O})\text{Fe}(\mu\text{-PDT})\text{Fe}(\text{CO})_2(\text{CN})]^{-1a}$

	2	3	4		2	3	4
Fe1	0.035	-0.240	0.088	C10	0.625	0.590 ^c	0.627
Fe2	-0.234	0.113	-0.136	O11	-0.452	-0.475	-0.463
S3	0.010	-0.032	-0.095	C12	0.651	0.506	0.645
S4	0.047	-0.013	-0.046	O13	-0.484	-0.452	-0.479
S5	-0.199	-0.136	-0.234	C14	0.029	-0.011	0.009
C6	0.029	0.076	-0.009	N15	0.471	-0.523	-0.491
N7	-0.528	-0.519	-0.545	O _{water}	-0.947	-0.892	-0.903
C8	0.537 ^b	0.617	0.589	H _{water} ^d	0.518	0.535	0.570
O9	-0.470	-0.486	-0.512				

^a Natural atomic charges computed at the minimum-energy geometry. The atom numbering is from Figure 1c. ^b Semibridged CO (see Figure 2). ^c Bridged CO (see Figure 2). ^d Average values for the two H atoms of the water ligand.

kinetic inaccessibility) of **4** with respect to **3** are more subtle and not so immediately evident from the available X-ray structures of Fe-only hydrogenases.^{2,3,10} It is also interesting to note that **4** does not have the right characteristics to be directly involved in H₂ binding within the catalytic cycle. In fact, the H₂O molecule bridging the two Fe(II) centers is expected to be very acidic, and the resulting hydroxo group can hardly be replaced by H₂.

$[(\text{CO})(\text{CH}_3\text{S})(\text{CN})\text{Fe}(\text{II})(\mu\text{-PDT})\text{Fe}(\text{II})(\text{CO})_2(\text{CN})]^{-1}$. The formation of catalytically active species, produced by the dissociation of ligands from parent complexes, occurs in many catalytic cycles involving organometallic complexes.^{20,21} In addition, Hall and co-workers^{9,11} have shown that only an Fe(II)Fe(II) redox form of the [2Fe]_H cluster can activate H₂. In this context, the Fe(II)Fe(II) complex $[(\text{CO})(\text{CH}_3\text{S})(\text{CN})\text{Fe}(\mu\text{-PDT})\text{Fe}(\text{CO})_2(\text{CN})]^{-1}$ (see Figure 1c) is expected to be a good model of the isolated [2Fe]_H cluster,

and because of its coordinative unsaturation, it is expected to bind and possibly activate H₂.

The search for the optimum geometry of the complex $[(\text{CO})(\text{CH}_3\text{S})(\text{CN})\text{Fe}(\mu\text{-PDT})\text{Fe}(\text{CO})_2(\text{CN})]^{-1}$ led to two distinct isomers (**5** and **6**, respectively, see Figure 3 and Table 3). The most stable form, **5**, which is formally derived from the reaction $\mathbf{2} \rightarrow \mathbf{5} + \text{H}_2\text{O}$ ($\Delta E = 19.7$ kcal mol⁻¹), is characterized by the two iron atoms that have (slightly distorted) square pyramidal coordination. The two pyramids share one edge of their bases, identified by the two S atoms of the bridging PDT ligand. The vicinal Fe1 atom also has a CN⁻ and a CH₃S⁻ ligand in the basal plane, whereas the corresponding ligands for the distal Fe2 are CN⁻ and CO, respectively. The CO axial ligands lie at opposite sides with respect to the least-squares plane Fe1–μS–μS–Fe2. This isomer is expected to be particularly stable because two CO groups out of three are characterized by vacant trans positions. It is also important to observe that the optimized structure of **5** differs considerably from the structure of the [2Fe]_H cluster that is found in the enzyme.^{2,3} In particular, the CH₃S⁻ ligand is equatorial in **5**, whereas the corresponding cysteine group is axial in the [2Fe]_H cluster. As mentioned above, this orientation of the CH₃S⁻ ligand is not compatible with the structure of the active site of Fe-only hydrogenases.

Another minimum-energy structure, **6**, is related to the precursor **3** according to the reaction $\mathbf{3} \rightarrow \mathbf{6} + \text{H}_2\text{O}$ ($\Delta E = 25.0$ kcal mol⁻¹). **6** lies 20.4 kcal mol⁻¹ higher in energy than does **5** and is structurally very similar to the [2Fe]_H

(20) Torrent, M.; Solà, M.; Frenking, G. *Chem. Rev.* **2000**, *100*, 439–493.

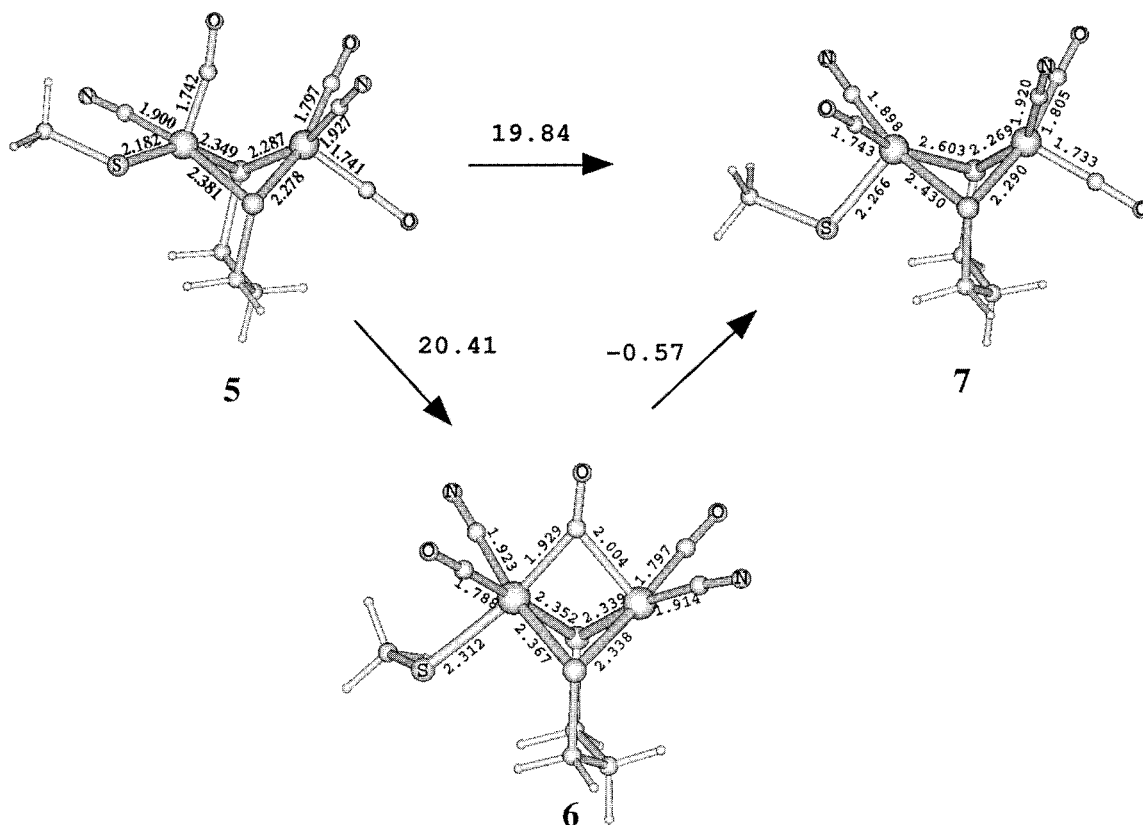


Figure 3. Optimized structures and relative energies of **5**, **6**, and **7**. Relevant bond distances are shown. Fe–Fe distances for **5**, **6**, and **7** are 2.686, 2.516, and 2.869 Å, respectively.

Table 3. Natural Atomic Charges of $[(\text{CO})(\text{CH}_3\text{S})(\text{CN})\text{Fe}(\mu\text{-PDT})\text{Fe}(\text{CO})_2(\text{CN})]^{-1a}$

	5	6	7	5	6	7
Fe1	-0.003	-0.218	0.132	O9	-0.471	-0.465
Fe2	-0.230	0.112	-0.153	C10	0.615	0.483 ^c
S3	0.037	-0.009	-0.107	O11	-0.453	-0.446
S4	0.037	-0.013	-0.005	C12	0.636	0.599
S5	-0.106	-0.088	-0.163	O13	-0.486	-0.454
C6	0.031	0.057	-0.006	C14	0.029	-0.019
N7	-0.517	-0.511	-0.507	N15	-0.479	-0.470
C8	0.549 ^b	0.640	0.613			

^a Natural atomic charges computed at the minimum-energy geometry. The atom numbering is from Figure 1c. ^b Semibridged CO (see Figure 3). ^c Bridged CO (see Figure 3).

cluster observed in the enzyme (see Figure 3 and Table 3). The hexacoordination of Fe1 is achieved via a μ_2 -CO ligand bridging the two iron centers, while the coordination of Fe2 is (pseudo) square pyramidal. In **6**, the $\text{CH}_3\text{S}-$ group is trans to the μ_2 -CO ligand, which behaves as a trans-weakening group, as indicated by the Fe–S distance increasing from 2.18 to 2.31 Å on going from **5** to **6**.

Among the hydrated forms, only **4** does not lead to a stable isomer. In fact, when structure optimizations are carried out starting from **4** and removing the water molecule, the cluster rearranges again to **5**. To verify to what extent the protein environment can influence the structure of the diiron cluster, a constrained optimization has been carried out with the dihedral angle $\text{CH}_3\text{S}-\text{Fe1}-\text{Fe2}-\text{CN}$ fixed to the position observed in **4**. The optimized structure **7** (see Figure 3) has axial groups ($\text{CH}_3\text{S}-$ for Fe1 and CO for Fe2)

on the same side of the least-squares $\text{Fe1}-\mu\text{S}-\mu\text{S}-\text{Fe2}$ plane and lies 19.8 kcal mol⁻¹ higher in energy than does **5**. Interestingly, **7** is about 0.6 kcal mol⁻¹ more stable than **6**, and the conversion **6** \rightarrow **7** is expected to occur with a low activation energy because it involves only the concerted movements of one μ_2 -CO and one μ_1 -CO ligand. As discussed below, this could have relevant implications on the catalytic properties of the bimetallic cluster.

$[(\text{CO})(\text{CH}_3\text{S})(\text{CN})(\text{H}_2)\text{Fe}(\text{II})(\mu\text{-PDT})\text{Fe}(\text{II})(\text{CO})_2(\text{CN})]^{-1}$. The coordination of H_2 to **5**, **6**, and **7** leads to **8**, **9**, and **10**, respectively (see Figure 4 and Table 4). In the three isomers, the H_2 moiety keeps its molecular character, and the computed H–H distances fall in the range 0.79–0.85 Å, whereas it is equal to 0.74 Å in the free H_2 molecule. In **8**, H_2 is bound to the vicinal Fe1 center and is trans to a CO group and the reaction energy for **5** + $\text{H}_2 \rightarrow$ **8** is equal to -4.7 kcal mol⁻¹. Coordination of H_2 to **6** leads to **9**, which is analogous to a proposed intermediate in the enzymatic cycle, in light of the experimentally derived structure of the $[\text{2Fe}]_{\text{H}}$ subcluster in the enzyme.^{4,10} The calculated reaction energy for **6** + $\text{H}_2 \rightarrow$ **9** is equal to -14.1 kcal mol⁻¹, which is in close agreement with that obtained by Hall and co-workers.⁹ In **10**, which is formally derived from **7** + H_2 and is a real isomer (no external constraints were applied), the H_2 molecule is bound to the vicinal Fe1 atom and is trans to the $\text{CH}_3\text{S}-$ ligand. The reaction energy is equal to -15.9 kcal mol⁻¹. Note that **10** is the only stable product derived from H_2 and **7**. Indeed, when the geometry optimization of **7** + H_2 is carried out with dihydrogen bound to Fe2, the

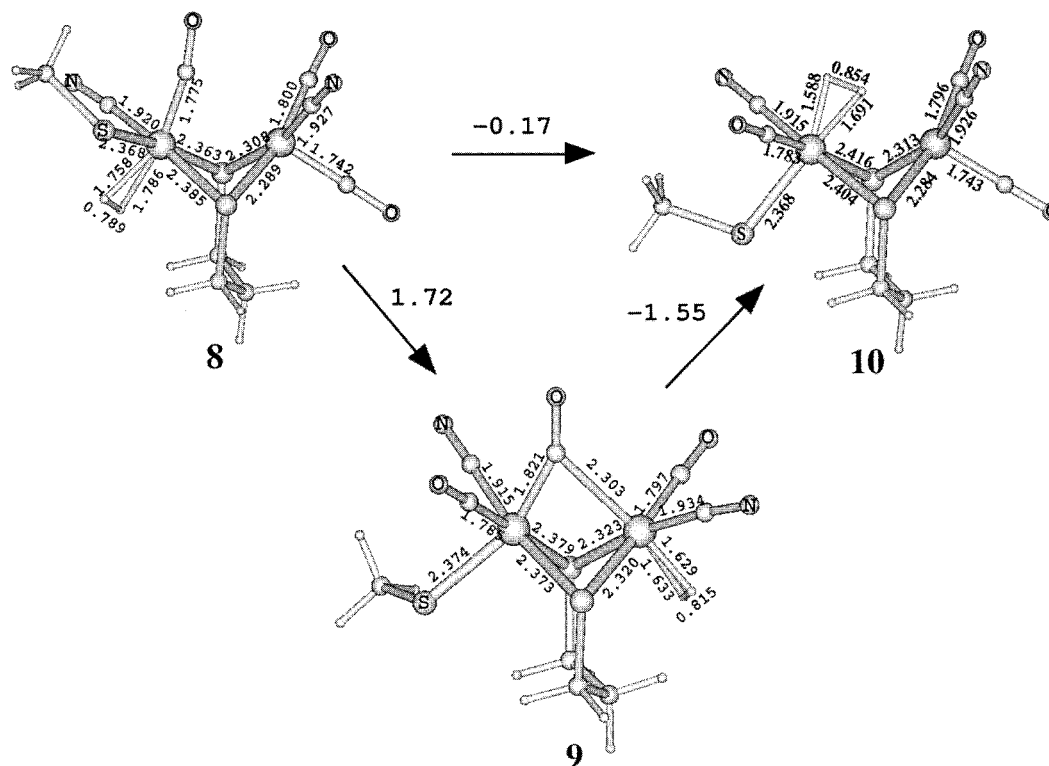


Figure 4. Optimized structures and relative energies of **8**, **9**, and **10**. Relevant bond distances are shown. Fe–Fe distances for **8**, **9**, and **10** are 2.659, 2.697, and 2.598 Å, respectively.

Table 4. Natural Atomic Charges of $[(\text{CO})(\text{CH}_3\text{S})(\text{CN})(\text{H}_2)\text{Fe}(\mu\text{-PDT})\text{Fe}(\text{CO})_2(\text{CN})]^{-1a}$

	8	9	10	11	12
Fe1	-0.137	-0.253	-0.227	-0.180	-0.171
Fe2	-0.201	-0.165	-0.263	-0.331	-0.338
S3	0.017	0.021	-0.002	0.068	0.251 ^b
S4	0.043	0.027	0.070	0.040	-0.014
S5	-0.154	-0.144	-0.166	-0.260	-0.267
C6	0.052	0.078	0.047	0.011	0.029
N7	-0.515	-0.512	-0.506	-0.407	-0.545
C8	0.549 ^c	0.623	0.616	0.671	0.668
O9	-0.461	-0.475	-0.478	-0.482	-0.496
C10	0.626	0.523 ^c	0.619	0.636	0.633
O11	-0.453	-0.441	-0.457	-0.466	-0.461
C12	0.645	0.614	0.647	0.622	0.609
O13	-0.484	-0.460	-0.481	-0.485	-0.484
C14	0.036	0.011	0.020	0.082	0.103
N15	-0.479	-0.491	-0.485	-0.499 ^d	-0.492
H	0.026	0.150	0.183	-0.052	-0.042 ^d
H	0.113	0.084	0.030	0.203 ^e	0.168 ^e

^a Natural atomic charges computed at the minimum-energy and transition-state geometries. The atom numbering is from Figure 1c. ^b Protonated (see Figure 5). ^c Semibridged CO (see Figure 4). ^d Bridged between the two metal centers. ^e Bonded to S3.

adduct spontaneously evolves to **10**, with H₂ coordinated to Fe1. The relative stabilities for the H₂ adducts **8**, **9**, and **10** are illustrated in Figure 4. Note that the large stability of **5** (the most stable parent compound) is partially lost in the reaction $\mathbf{5} + \text{H}_2 \rightarrow \mathbf{8}$, which is less exothermic by about 10 kcal mol⁻¹ than the corresponding reactions for **6** and **7**. As a consequence, **8**, **9**, and **10** have very similar stabilities and are expected to coexist at thermal equilibrium. A possible origin of the different exothermicities of the H₂ binding reactions and, consequently, of the small energy differences observed among **8**, **9**, and **10** can be explained by considering

that CO groups in these isomers experience very similar coordination environments and similar trans influences (see Figure 4). It is worth noting that in **8** the presence of a CO trans to H₂ leads to a H₂–Fe distance that is longer than the distances in **9** and **10** by about 0.1 Å. Correspondingly, the H–H distance in **8** is shorter by 0.03–0.06 Å, indicating a relatively weak activation of H₂. Note also that in **9** the bridging CO is trans to H₂ but is shifted toward Fe1, thus reducing its influence on the H₂ coordination at Fe2. In addition, the analysis of NAO charges for **8**, **9**, and **10** (see Table 4) reveals that H₂ is more polarized in **10** than in **8** and **9**.

Catalytic Properties of $[(\text{CO})(\text{CH}_3\text{S})(\text{CN})\text{Fe}(\text{II})(\mu\text{-PDT})\text{Fe}(\text{II})(\text{CO})_2(\text{CN})]^{-1}$ Isomers. The structures and electronic properties of **2**–**10** prompted us to explore possible mechanisms of H₂ activation as promoted by $[(\text{CO})(\text{CH}_3\text{S})(\text{CN})\text{Fe}(\mu\text{-PDT})\text{Fe}(\text{CO})_2(\text{CN})]^{-1}$ complexes. Hall and co-workers⁹ recently showed that the activation of H₂ by a species analogous to **9** is not possible. In particular, the cleavage of H₂ on the distal Fe2 atom followed by the protonation of a μ₂-S ligand is associated with an activation energy that is higher than 17 kcal mol⁻¹, and the product is 15.3 kcal mol⁻¹ less stable than the starting H₂ complex.⁹ On the other hand, proton transfer to one of the CN⁻ ligands is associated with a much higher barrier (37.8 kcal mol⁻¹), even if the product is slightly more stable (–0.3 kcal mol⁻¹) than the dihydrogen complex.⁹ Interestingly, if the PDT group in **9** is substituted by DTMA, the activation of H₂ and the transfer of a H⁺ ion to the N atom of DTMA becomes an accessible pathway for H₂ cleavage.¹¹ However, the presence of the

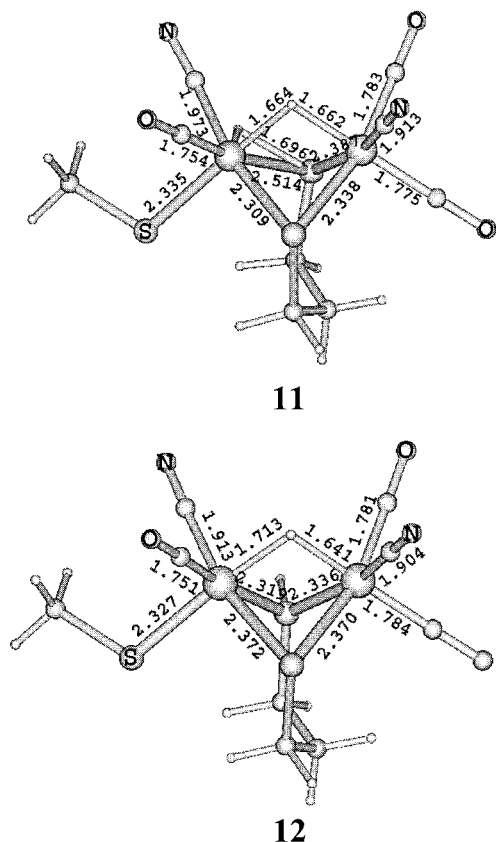


Figure 5. Optimized structures of **11** and **12**. Relevant bond distances are shown. Fe–Fe distances for **11** and **12** are 2.600 and 2.687 Å, respectively.

DTMA ligand in the $[2\text{Fe}]_{\text{H}}$ cluster has not been proved experimentally.

In **10**, the H_2 molecule is coordinated to Fe1 and, in principle, could undergo heterolytic cleavage, resulting in the transfer of H^+ to a $\mu_2\text{-S}$ atom of PDT and of H^- to a bridging position between the two metal centers. Indeed, our calculations show that this pathway is very favorable for H_2 activation. The energy barrier from the reactant **10** to the transition state (TS) **11** is equal to $5.3 \text{ kcal mol}^{-1}$, and the final reaction product **12** is only $2.4 \text{ kcal mol}^{-1}$ less stable than **10** (see Figure 5). H_2 dissociation is accompanied by relatively small geometric rearrangements of the bimetallic cluster: the Fe–Fe bond distance is 2.697 \AA in **10**, 2.600 \AA in **11**, and 2.687 \AA in **12**. In **11**, the H_2 molecule is considered to be completely dissociated, with a H–H distance equal to 2.404 \AA . Correspondingly, the H–S distance is reduced to 1.696 \AA . In **12**, the S–H bond distance is 1.355 \AA , and the two hydrogen atoms are 3.456 \AA apart. $\mu_2\text{-H}$ coordination between the two Fe atoms is characterized by Fe1–H = 1.713 \AA and Fe2–H = 1.641 \AA bond distances.

Another chemical characterization of H_2 dissociation can be made on the basis of the NAO net atomic charges. The heterolytic character of the H_2 cleavage is evident from the change of the atomic charges observed in **10** and **12** (see Table 4). In **12**, the bridging H atom has some hydride character, whereas the H atom bound to the S ligand acquires a significant positive charge. In addition, the electron density on the distal Fe2 atom increases (because of the charge

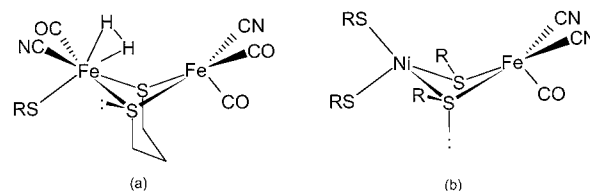


Figure 6. (a) Schematic structure of $[(\text{CO})(\text{CH}_3\text{S})(\text{CN})(\text{H}_2)\text{Fe}(\mu\text{-PDT})\text{-Fe}(\text{CO})_2(\text{CN})]^-$ (**10**). (b) Schematic structure of the [NiFe] hydrogenase active site as deduced by X-ray diffraction.²⁶ The spatial orientations of one lone pair of bridging S atoms are explicitly highlighted.

transfer from the hydride ion) and correspondingly decreases on the proximal Fe1. Interestingly, the structure of **12** is similar to that of a proposed intermediate species generated from H_2 activation that is catalyzed by [NiFe] hydrogenases, where a H atom bridges the two metal centers.^{22–24} However, when considering [NiFe]-hydrogenases, the S atom that is proposed to act as a base in the heterolytic cleavage of H_2 is derived from one of the terminal cysteine residues coordinated only to the Ni center. In fact, DFT investigations have shown that the protonation of the bridging cysteine residues in [NiFe]-hydrogenase models is energetically unfavorable and results in unrealistic modifications of the structure of the bimetallic cluster.²⁴ The different behavior of the $\mu_2\text{-S}$ atoms observed in models of [NiFe]-hydrogenase and in the complexes investigated in the present study is essentially due to the structural properties of the bimetallic clusters. In fact, because of the structural characteristics of the PDT ligand and by assuming that a simplified picture based on localized hybrid orbitals is applicable, one can observe that the orientation of the sp^3 orbital describing the $\mu_2\text{-S}$ lone pair in **10** (and in all other complexes investigated in the present study) is equatorial with respect to the least-squares plane Fe1– μS – μS –Fe2 (see Figure 6a). However, in the active site of [NiFe]-hydrogenases, the $\mu_2\text{-S}$ lone pairs are axial (see Figure 6b),²⁵ making them unsuitable for favorable interaction with the incoming H_2 molecule.

To complete this study, we have also investigated the activation of H_2 starting from **8** (see Figure 7), although, as discussed above, this reaction path hardly plays a role within the enzyme because of the peculiar coordination environment of the Fe1 center. However, the path could have some relevance to synthetic complexes. According to our calculations, the conversion $\mathbf{8} \rightarrow \mathbf{13}$ is endothermic by only $1.0 \text{ kcal mol}^{-1}$, but the activation energy ($10.7 \text{ kcal mol}^{-1}$) is more than 5 kcal mol^{-1} higher than that of the corresponding $\mathbf{10} \rightarrow \mathbf{12}$ reaction.

- (21) Saillard, J.-Y.; Hoffmann, R. *J. Am. Chem. Soc.* **1984**, *106*, 2006–2026 and references therein.
- (22) Niu, S.; Thomson, L. M.; Hall, M. B. *J. Am. Chem. Soc.* **1998**, *121*, 4000–4007.
- (23) De Gioia, L.; Fantucci, P.; Guigliarelli, B.; Bertrand, P. *Inorg. Chem.* **1999**, *38*, 2658–2662.
- (24) Pavlov, M.; Siegbahn, P. E. M.; Blomberg, M. R. A.; Crabtree, R. H. *J. Am. Chem. Soc.* **1998**, *120*, 548–555. Pavlov, M.; Blomberg, M. R. A.; Siegbahn, P. E. M. *Int. J. Quantum Chem.* **1999**, *73*, 197–207. De Gioia, L.; Fantucci, P.; Bienati, M. In *Recent Advances in Density Functional Methods*; Chong, D. P., Ed. In press.
- (25) Volbeda, A.; Charon, M.-H.; Piras, C.; Hatchikian, E. C.; Frey, M.; Fontecilla-Camps, J. C. *Nature* **1995**, *373*, 580–584.

Scheme 1. Plausible Pathways for H₂ Binding and Activation in Which the Energy Differences (kcal mol⁻¹) Associated with the Reaction Steps Are Reported

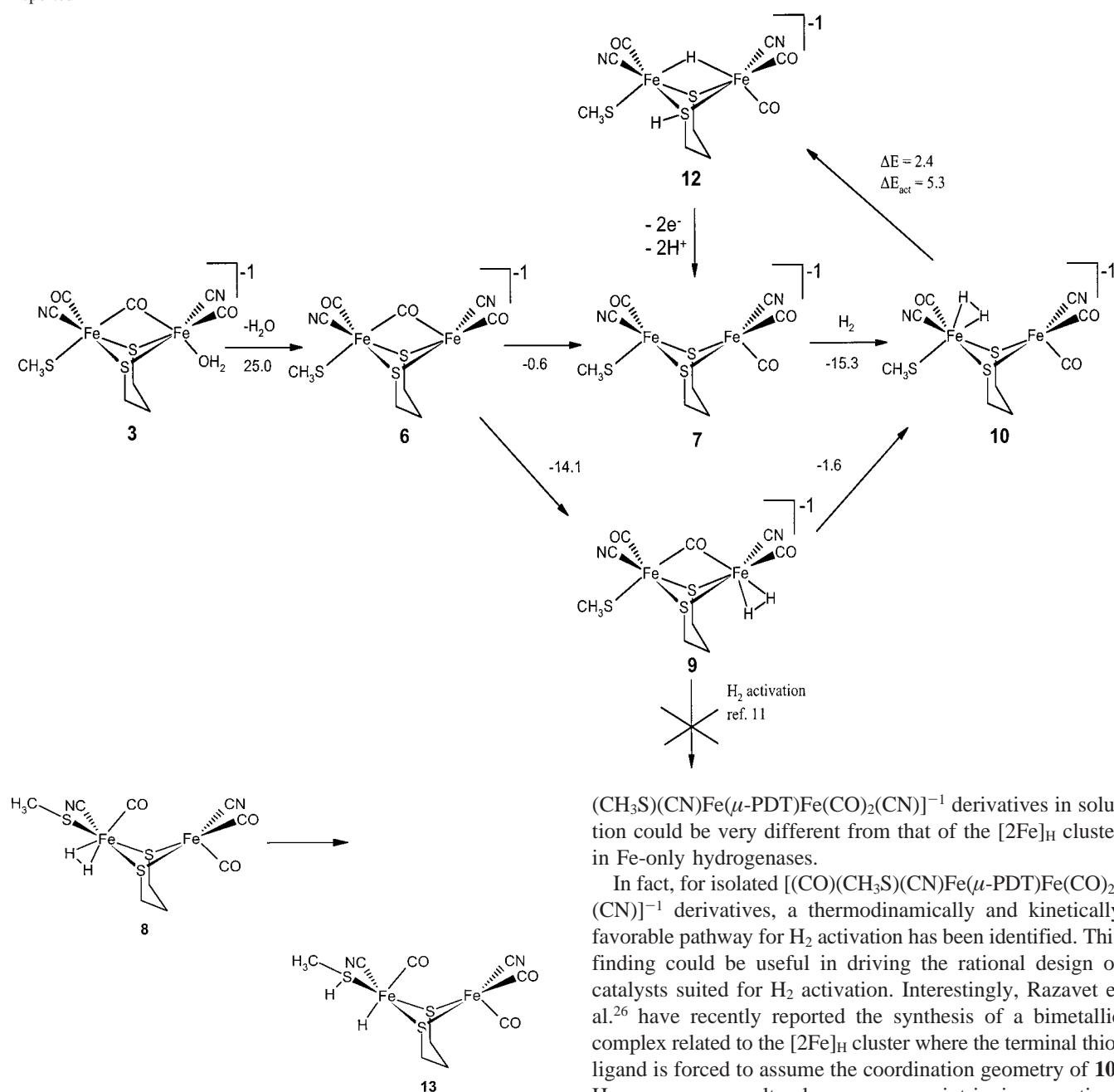


Figure 7. Schematic structure of optimized **8** and **13**.

Conclusions

The present DFT investigation of [(CO)(CH₃S)(CN)Fe(μ-PDT)Fe(CO)₂(CN)]⁻¹ isomers and of their H₂O and H₂ adducts has produced a number of interesting new observations.

The structure of the [(CO)(CH₃S)(CN)(H₂O)Fe(μ-PDT)Fe(CO)₂(CN)]⁻¹ cluster observed in the enzyme does not correspond to the absolute energy minimum when the protein is not explicitly taken into account. This result could imply that the Fe(II)Fe(II) redox state does not correspond to the oxidized form of the enzyme or, more probably, that the protein is able to constrain the specific coordination arrangement of the cluster. As a result, the chemistry of free [(CO)-

(CH₃S)(CN)Fe(μ-PDT)Fe(CO)₂(CN)]⁻¹ derivatives in solution could be very different from that of the [2Fe]_H cluster in Fe-only hydrogenases.

In fact, for isolated [(CO)(CH₃S)(CN)Fe(μ-PDT)Fe(CO)₂(CN)]⁻¹ derivatives, a thermodynamically and kinetically favorable pathway for H₂ activation has been identified. This finding could be useful in driving the rational design of catalysts suited for H₂ activation. Interestingly, Razavet et al.²⁶ have recently reported the synthesis of a bimetallic complex related to the [2Fe]_H cluster where the terminal thiol ligand is forced to assume the coordination geometry of **10**. However, our results also pose some intriguing questions concerning the catalytic activity of Fe-only hydrogenases. Scheme 1 shows two possible competing pathways for H₂ binding and activation starting from isomer **3** (i.e., the structure of the bimetallic cluster observed in the enzyme). The first step is common to the two pathways and is associated with the cleavage of the Fe–H₂O bond. As expected, this step is strongly endothermic and could imply that the one-electron reduction of the Fe(II)Fe(II) cluster is a necessary step to the dissociation of water.²⁷ Besides, it is reasonable to expect that less strongly coordinating solvents

(26) Razavet, M.; Davies, S. C.; Hughes, D. L.; Pickett, C. J. *Chem. Commun.* **2001**, 847–848.

(27) Actually, Hall et al.⁹ suggested that the Fe(II)Fe(II) [2Fe]_H-H₂O complex is first reduced to Fe(II)Fe(I). This redox form releases H₂O and binds H₂ and is then oxidized back to an Fe(II)Fe(II) [2Fe]_H-H₂ species that is able to activate H₂.

could be displaced more easily by H₂. In any case, the product of H₂O dissociation (**6**) can either bind H₂ to the vacant coordination site, forming **9**, or rearrange to **7** and bind H₂, forming **10**. A crucial point is that the **6** → **7** → **10** pathway is thermodynamically more favored (and expected to be kinetically facile, at least considering the isolated complexes²⁸) than the **6** → **9** pathway. In addition, the H₂ activation on **10**, as we have shown in the present study, can take place easily without the involvement of any heteroatom on the S–X₃–S bridging ligand, whereas the activation on **9** necessarily implies the presence of a DTMA (or similar) bridging ligand, as shown by Hall et al.¹¹ The reaction **3** + H₂ → **10** + H₂O, which as been described in Scheme 1

(28) Dance, I. *Chem. Commun.* **1999**, 1655–1656.

as a purely dissociative step followed by H₂ binding, could be, in fact, a concerted reaction that is endothermic by only about 9 kcal mol⁻¹. Of course, the **6** → **7** conversion could be kinetically disfavored within the enzyme. In any case, our results pose new and interesting questions concerning the catalytic mechanism of Fe-only hydrogenase, and further experimental and theoretical studies are necessary to clarify these aspects.

Supporting Information Available: Listings of the total molecular energies computed for the [(CO)(CH₃S)(CN)(H₂O)Fe-(μ-PDT)Fe(CO)₂(CN)]⁻¹ isomers and their derivatives. This material is available free of charge via the Internet at <http://pubs.acs.org>.

IC010770R